A&A manuscript no.
(will be inserted by hand later)

Your thesaurus codes are:
04 (11.05.2; 08.06.2; 09.07.1; 11.09.4)

ASTRONOMY
AND
ASTROPHYSICS
24.1.1995

Self-regulated star-formation in chemodynamical models of galaxies

J. Köppen, Ch.Theis, G.Hensler

Institut für Theoretische Physik und Sternwarte, Olshausenstr.40, D-24098 Kiel, Germany

[the date of receipt and acceptance should be inserted later]

Abstract. We study numerically and analytically the evolution of galactic stellar and gaseous components in a closed-box model that includes the energetics of the star-forming gas. The gas is heated mainly by massive stars (UV-radiation, stellar winds, type II supernovae). The stellar birth function depends on the density (g), but also on the temperature of the gas. This describes the fact that the star-forming molecular fraction is smaller in hot and warm gas than in cold clouds. This negative feed-back causes the system to exhibit a strong self-regulation, quite independent of the parametrizations of the basic processes. The resultant eqilibrium star-formation rate is a quadratic Schmidt-type law (SFR $\propto g^2$), independent of the assumed form and parameters of the stellar birth function. An analysis of the local and global stability shows that this behaviour is stable against disturbances in the state of the interstellar medium as well as against reasonable changes in the parametrizations of the star-formation or heating processes. While low or high gas densities the system reaches the equilibrium directly, at intermediate densities ($10^{-3.5} - 10^{-1}$M$_\odot$pc^{-3}) it performs strongly damped oscillations. In any case, a system settles into equilibrium within a short time (the cooling time of the gas), and evolves almost exclusively in equilibrium.

Key words: – galaxies: chemical evolution – ISM: star formation

1. Introduction

To understand the (chemical) history of galaxies, one must know the star-formation rate (SFR), preferably dependent on all the relevant physical parameters. To compute this rate from first principles has so far been impossible, because it would require that we completely understand the formation of stars of all masses.

Thus, a more phenomenological approach has to be taken: In models of the chemical evolution of galaxies, one often assumes that the SFR is a function which depends on a power of the local gas density (cf. Schmidt, 1959); usually this power is around 1 or 2. This choice is quite reasonable, since young stars and candidates for protostars are usually found in regions of high density and low temperature, such as molecular clouds. However, it still is subject to debate (or taste) which exponent one uses, whether one uses the space density or the surface density, or rather the density of the gas in molecular form (cf. Larson 1982, Rana & Wilkinson 1986).

Evolutionary and population synthesis models that reproduce the observed chemical and photometric properties of galaxies clearly indicate that the SFR is quite different in galaxies and stellar populations of different morphological types (e.g. Sandage 1986, Table 1 of Köppen & Arimoto 1990): spheroids of disk galaxies and elliptical galaxies are thought to have been formed long ago within a relatively short time ($\tau_{\rm SFR} \approx 0.1$ Gyr). In the disks of spiral galaxies star-formation still is going on ($\tau_{\rm SFR} \approx 3$ Gyr for the solar neighbourhood). In irregular galaxies the SFR is still lower: Hunter & Gallagher (1985) showed that $\tau_{\rm SFR}$ exceeds the Hubble time in dwarf irregulars. However, these models cannot tell us the physical reason for this difference. Is there an universal prescription for the SFR, or are the physical processes that determine star-formation genuinely different in ellipticals and disk galaxies?

Several studies show that star-formation may be the result of a self-regulation due to the stars depositing energy and momentum into the neighbouring gas: this can be ionizing photons (Cox 1983) or stellar winds (Franco & Cox 1983, Franco & Shore 1984), balanced by cloud energy losses. Such a balance is the basis of Dopita's (1985) parametrized SFR, which is fitted to observations (Donas et al. 1987). Firmani & Tutukov (1992) consider the global balance of the gas turbulent energy. These studies explore possible scenarios, and lead to attractively simple SFR prescriptions, however they *assume* the existence of an equilibrium between the processes considered, and do not show that they are the result of physically consistent description of the gas-star system, and which of the processes dominate.

Our chemodynamical approch to evolution of galaxies (Hensler 1987, Theis et al. 1992) tries to describe as precisely as possible the known physical processes occuring in the interstellar medium and its interaction with the stars. In this manner, one avoids as much as possible ad hoc assumptions or

Send offprint requests to: J. Köppen

descriptions with unknown parameters. However, one ad hoc assumption seems to remain: The stellar birth function (SBF). But, experience with this type of models has shown that under common conditions the system enters a mode of self-regulated star-formation. When this happens, the star-formation rate becomes quite independent of the assumed parameters describing the SBF. With this single (universal) star formation recipe it is possible to explain the structure and properties of elliptical galaxies (Theis et al. 1992) as well as bulges and disks (Samland et al. 1994).

Since the full chemodynamical models with their complete network of mass and energy transfer processes require a very large numerical computational effort, it has not been possible to perform a complete examination and thorough analysis of the behaviour of the system. In particular it is necessary to determine how (in)sensitive the results depend on the adopted prescriptions, and to find the crucial parameters. Likewise, one wishes to know under which physical conditions self-regulation occurs. In this paper we investigate this in detail by considering a simplified network of processes which is described in Sect. 2. For the equilibrium state an analytical solution can be found (Sect. 3) whose sensitivity on all parameters is studied. In Sect. 4 we perform a local (linear) stability analysis. The global behaviour of the solutions is investigated in Sect. 5. Implications of these results and comparison with observations are discussed in Sect. 6.

2. The model

2.1. Units

Throughout this paper, we shall use the units parsec, 10^6 years, and solar masses.

2.2. The Equations

Even though the complete system of interactions and processes in the formulation of Theis et al. (1992) is rather complex, experience suggests reasonable results for a wide range of models that encorporate a smaller number of processes. We chose a partial model, which tries to keep some essential features, but involves only one gas phase and one stellar type: We consider a closed box system in which at the beginning all matter is in the form of gas. From the gas, both massive and less massive stars are formed with a rate that depends not only on gas density, but also on gas temperature via an efficiency factor. This factor is meant to describe what fraction of the gas is in the form of star-forming molecular clumps. While the less massive stars are assumed to have no further influence on the interstellar medium and simply accumulate as ‘remnants’, the massive stars are assumed to be responsible for the heating of the gas.

In this scenario, the temporal evolution of the mass densities of gas (g), massive stars (s), and remnants (r) are described by

$$\frac{dg}{dt} = -\Psi(g,T) + \eta s/\tau \qquad (1)$$

$$\frac{ds}{dt} = \xi\Psi(g,T) - s/\tau \qquad (2)$$

$$\frac{dr}{dt} = (1-\xi)\Psi(g,T) + (1-\eta)s/\tau. \qquad (3)$$

The gas is decreased due to star formation by a rate $\Psi(g,T)$ which we shall refer to as the *stellar birth function* (SBF). The gas is replenished by the matter returned from the massive stars after their lifes. ξ is the mass fraction of freshly formed massive ($m > 10 M_\odot$) stars, which amounts to 0.12, if one considers a Salpeter IMF between the mass limits 0.1 and 100 $M_\odot$. The fraction η of how much gas is ejected into the ISM by the massive stars is taken to be 0.9, if one uses a mass of 1.4 $M_\odot$ for the resulting remnant. The finite lifetime of the stars is treated in an approximate way by assuming that the gas return follows a time constant proportional to the mean stellar lifetime of τ = 10 Myr.

The SBF is given by a power law dependence on gas density and an efficiency factor which depends on the gas temperature

$$\Psi(g,T) = C_n g^n f(T) \qquad (4)$$

Theis et al. (1992) use a quadratic law ($n = 2$ and $C_2 = 0.55$ which is the prescription of Larson 1969), and an efficiency factor which is unity below 100 K, zero above 10000 K, with a suitable interpolation in between. Another, merely formal difference is that they apply the efficiency factor to the gas fraction itself rather than the SBF.

Here, we shall treat all parameters as being free. For the form of the efficiency factor we chose an exponential function

$$f(T) = e^{-T/T_s} \qquad (4a)$$

with a constant T_s = 1000 K which gives the same principal features of the formulation by Theis et al. but also is continuously differentiable.

The internal energy density of the ISM ($e = 1.5 k_B g T/m =: bgT$ with Boltzmann's constant k_B and the mean molecular weight m of the interstellar gas; b = 0.013 in our units)

$$\frac{de}{dt} = h(g)s - g^2\Lambda(T) \qquad (5)$$

is increased by the heating from the stars and is diminished by the radiative cooling of the gas. In the general ISM, most of the energy is in the form of cloud motions, as there is usually little exchange between thermal and kinetic energy. The dynamical state of a star-forming cloud does not affect its degree of fragmentation and therefore its SBF. This might change in the case of a strong interaction (stellar outflows) or collision of clouds. However, Hausman (1981) showed that the dissipated energy is radiated away quickly, so that in a first order approximation the average cloud temperature is not changed by cloud-cloud collisions. This pertains especially to the small-scale star-forming regions with their higher densities.

We consider two cases for the heating-rate coefficient h:

a) h is constant, if all the energetic photons of the stars or all the mechanical energy which they impart on the ISM via their winds are absorbed in the gas, and the heating rate is proportional only to the density of stars.

b) $h(g) \propto g$ for heating by absorption of stellar photons in an optically thin gas.

The coefficient for heating by absorption of Lyman continuum photons is given by

$$h = \eta_{\rm LyC} E_{\rm LyC} \frac{\int L_{\rm LyC}\phi(m)dm}{\int m\phi(m)dm}$$

where both integrations involve the initial mass function $\phi(m)$ and extend over the mass range (10 to 100 $M_\odot$) of the stars responsible for this radiation. $E_{\rm LyC} \approx 13.6$ eV is the average photon energy. Following Hensler & Burkert (1989) we use a stellar Lyman continuum luminosity of

$$L_{\rm LyC} = 10^{40}\,(m/{\rm M}_\odot)^6 \quad {\rm photons\,s^{-1}star^{-1}}$$

The efficiency factor $\eta_{\rm LyC}$ for the conversion of absorbed photon energy into thermal energy was set to 10^{-4}, well within the range of values discussed by Tenorio-Tagle et al. (1986). This gives a value of $h = 21900$ in our units.

The radiative cooling is taken as the standard interstellar cooling curve, i.e. described by a temperature dependent cooling function $\Lambda(T)$ (Böhringer & Hensler, 1987). Since this function mainly increases with increasing temperature, one has approximately:

$$\Lambda(T) = \Lambda_0\,(T/10000\ {\rm K})^\lambda \tag{6}$$

For the calculations presented here, we use the piecewise approximation of Hensler (1987) in the temperature range $10^2 < T < 10^4$ K : The cooling rate per atom is $4 \cdot 10^{-28} T^{0.5}$ erg cm^3 s^{-1} which gives $\lambda = 0.5$ and for cooling coefficient per unit gas mass $\Lambda_0 = 1800\ \ {\rm M}_\odot{}^{-1}{\rm pc}^3{\rm Myr}^{-3}$ in our units.

3. The equilibrium solution

3.1. A first-order approach

To compute the equilibrium, one can simplify the equations even further: For very short stellar lifetimes τ one may assume stationarity of the stellar fraction, which gives for density of massive stars simply

$$s = \Psi(g,T)\xi\tau \tag{7}$$

Then one needs to consider only the system

$$\frac{dg}{dt} = -(1-\xi\eta)\Psi(g,T) \tag{8a}$$

$$\frac{de}{dt} = h\xi\tau\Psi(g,T) - g^2\Lambda(T) \tag{8b}$$

For simplicity, we also had assumed the case $h(g) = const.$ for the ISM heating. Inspecting the characteristic timescales, one finds for the first equation

$$\frac{g}{|dg/dt|} = \frac{\tau_{\rm SFR}}{1-\xi\eta} \tag{9}$$

essentially the star-formation timescale $\tau_{\rm SFR} = g/\Psi$, which is of the order of Gyrs in the solar neighbourhood. For the energy density equation,

$$\frac{e}{|de/dt|} = |\frac{1}{\tau_{\rm heat}} - \frac{1}{\tau_{\rm cool}}|^{-1} \tag{10}$$

the heating timescale

$$\tau_{\rm heat} = \frac{bgT}{h\Psi\xi\tau} = \frac{bT}{h\xi\tau}\tau_{\rm SFR} = 4.9\,10^{-4}\tau_{\rm SFR} \tag{11}$$

and the cooling timescale

$$\tau_{\rm cool} = \frac{bT}{g\Lambda} = 0.023\Psi/g^2\tau_{\rm SFR} = 4.6\,10^{-3}\tau_{\rm SFR} \tag{12}$$

are involved. The numerical expressions are obtained by using the parameter values for our 'standard' model, as given above, and a gas temperature of 1000 K. Thus, the timescales for heating and also for cooling, are much shorter than the characteristic timescale for the change of the gas density. Note that for a quadratic SBF, the ratio of $\tau_{\rm cool}/\tau_{\rm SFR}$ is independent of gas density, i.e. it remains small for all densities.

Assuming that the system always is in thermal balance ($de/dt = 0$), the equilibrium SFR can directly be computed from Eq. (8b):

$$\Psi_e(g,T_e) = g^2\frac{\Lambda(T_e)}{h\xi\tau} \tag{13}$$

If, as in our standard formulation, the cooling function has a weaker temperature dependence than the SBF efficiency factor, the equilibrium SFR is a quadratic function of the gas density, *irrespective* of how the assumed SBF depends on density, and whether it is a product of a temperature and a density dependent part.

With the known functional form of the assumed SBF $\Psi(g,T)$ the equilibrium temperature T_e can be obtained from this non-linear equation according to Eq. (4)

$$\frac{f(T_e)}{\Lambda(T_e)} = \frac{g^{2-n}}{h\xi\tau C_n} \tag{14}$$

which is solved by a one-point iteration or a bisection method. One notes that for a quadratic density dependence of Ψ, the equilibrium temperature is independent of gas density, and so the equilibrium SFR is strictly a quadratic function of density. Since the left hand side is a function that decreases with temperature, for a linear SBF ($n = 1$) the equilibrium temperature will be higher for lower gas densities. As the cooling function depends on temperature only weakly, this temperature rise leads to only a slight increase of the equilibrium SFR (see below, cf. Fig. 2).

3.2. Solution of the whole system

Let us now consider the full system (Eqs. (1) to (5)): As before, from inspection of the timescales, we can assume that thermal equilibrium is quickly established ($de/dt = 0$). This condition means that the ratio $x := s/g^2$ of star and gas densities is just a function of the equilibrium temperature according to Eq. (5)

$$x_e = \Lambda(T_e)/h. \tag{15}$$

As before, we consider an ISM heating rate h independent of g. Let us investigate whether the system has any critical points in the (x,e)-plane, i.e. where both variables do not change: $de/dt = 0$ and $dx/dt = 0$ simultaneously. Using Eqs.(1) and (2), one gets

$$\frac{dx}{dt} = \frac{\Psi}{g^2}(\xi + 2xg) - \frac{x}{\tau}(1 + 2xg\eta) \tag{16}$$

from which we see that such a critical point can exist, and that the equilibrium SFR is

$$\Psi_e(g, T_e) = g^2 \frac{x_e}{\xi\tau} \frac{1 + 2x_e g\eta}{1 + 2x_e g/\xi} \tag{17}$$

At low gas densities, the last factor on the right hand side becomes unity, and one recovers Eq. (13). For high densities, one gets

$$\Psi_e(g, T_e) = g^2 \frac{x_e\eta}{\tau} \tag{18}$$

We note that in both limiting cases, Ψ_e depends strictly on g^2, which means that the equilibrium temperature T_e (cf. Eq. 14) will be constant, if a SBF with a quadratic dependance on g (Eq. 4) had been assumed.

3.3. Properties of the equilibrium

Equations 1 to 5 can easily be integrated numerically. A simple trapezoidal rule is used, and the time step is adjusted automatically, so that the densities and the temperature do not change during any time step by more than a specified amount (usually 2 percent).

Figure 1 depicts the evolution of a few representative models with Ψ based on $n = 2$ in Eq. (4) and different values of the initial gas density, together with the equilibrium solutions obtained from Eqs. 4, 15, and 17. We show the ratio $\Psi(g, T)/g^2$, i.e. the deviation of the actual SFR from a quadratic dependence on gas density, as a function on gas density. Starting with a gas temperature of 10^4 K and zero stellar density, all the models reach the equilibrium within a relatively short time, approximately the cooling timescale. This early evolution shows up as a spike, which results from a brief period of higher star formation. While this episode is rather unimportant for the system at low initial densities, in the model with $\log(g_0) = 0.5$ the gas is cooled to very low temperatures, star-formation occurs at maximum efficiency, and the SFR is almost equal to the SBF for $T = 0$. This initial epoch is very short (a few star-formation timescales of about 1 Myr), during which about 50 percent of all the long-lived stars and remnants are formed. Details of this early evolution are discussed in Sect. 6. However, we note that at densities higher than about 1 $M_\odot pc^{-3}$ the SFR timescale is comparable or even shorter than the lifetime of the most massive stars, so that our description of the processes is probably no longer valid. Hence, we consider this part of the diagrams merely as an extrapolation of our simple description.

Figure 1 demonstrates that the analytical solution describes the equilibrium state of the numerical models precisely. Thus, one can well use the equilibrium solution directly, and avoid the additional computational effort for a time-dependent solution.

As expected from Eqs. (14) and (17), the equilibrium SFR has a strictly quadratic dependence on gas density for low densities. At high densities, the solution goes towards the other extreme case (Eq. 18), almost a factor of 10 lower than extrapolated from the low-density part. At the steepest part (near $\log(g) = 0$) one has about SFR $\propto 1.6$. If one were to interpret the behaviour of this self-regulated system by a simple power-law SFR, systematic differences between low and high densities could result. However, since this high-density branch of the solution implies star-formation timescales shorter than about 30 Myr, any system would pass through this regions quickly.

The actual level of SFR/g^2 is rather insensitive to the assumed factor of proportionality C_2 of the SBF: varying it from 0.1 to 10^{10} changes the self-regulated SFR by only a factor of 3. This is due to negative feed-back of the stellar heating via the temperature dependent efficiency factor in the SBF. However, for small values of the constant C_2, the star formation and hence the heating of the gas are at a very low level. Because the resulting gas temperature is close to zero, the star-formation efficiency factor $f(T) \approx 1$ is constant. Hence, the self-regulation mechanism obviously would not work any longer.

Figure 2 shows the equilibrium solutions, but done for an assumed linear SBF ($n = 1$). We do not plot any results from numerical models, because these exhibit the same excellent agreement as in Fig. 1. The deviation of the equilibrium SFR from a truly quadratic dependence on g is very slight indeed. Towards low densities, the ratio SFR/g^2 rises like $g^{0.05}$. This is due to the rising equilibrium temperature T_e, as discussed in Sect. 3.1. Just as with the quadratic SBF, the value for SFR/g^2 is quite insensitive to the assumed constant C_1. Comparison with Fig. 1 demonstrates that it is also insensitive to n, i.e. how strongly the assumed SBF depends on gas density — provided the star-formation is sufficiently large to ensure proper operation of the self-regulation mechanism.

In Fig. 3 we show how the behaviour of the self-regulated SFR depends on the power n. In the low-density limit one notes that for $n < 2$ the equilibrium temperature rises with decreasing gas density, as is discussed in connection with Eq. (14). For $n > 2$ the temperature decreases as the gas density is lowered. When it becomes too low, the self-regulation ceases to work: Though the star-formation efficiency is unity, the actual rate $\propto g^n$ is very small, because of the low density and the large exponent n. For larger values of C_n, self-regulation can operate over a larger range in densities, and the resultant SFR is at the same level as for smaller values of n.

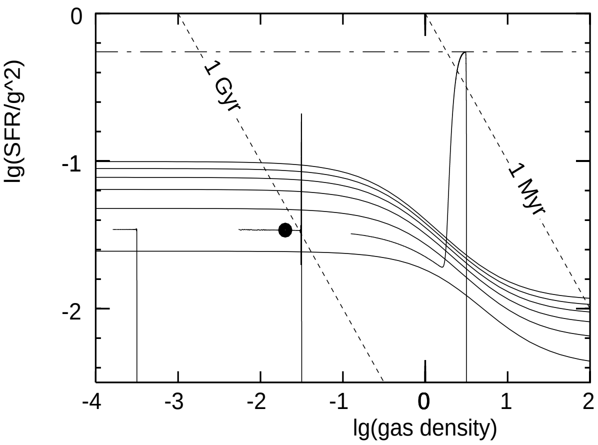

Fig. 1. The ratio SFR/g^2 of the actual star-formation rate and gas density as a function of the gas density g: shown are the analytical equilibrium solutions for various values of the constant in the SBF ($\log(C_2)$ = 9, 7, ... , -1 from top to bottom). Also depicted are results from three numerical models with initial gas densities of $\log(g)$ = 0.5, -1.5, and -3.5 for an assumed stellar birth function SBF of $\Psi = 0.55 g^2 f(T)$. The dot-dashed line indicates the value for maximum efficiency (for T = 0). Along the short-dashed lines the star-formation timescale is equal to 1 Myr and 1 Gyr. The filled dot marks the equilibrium for the 'standard' value $C_2 = 0.55$ at the density of the local interstellar medium ($n_{\rm gas}$ = 1 cm^{-3}).

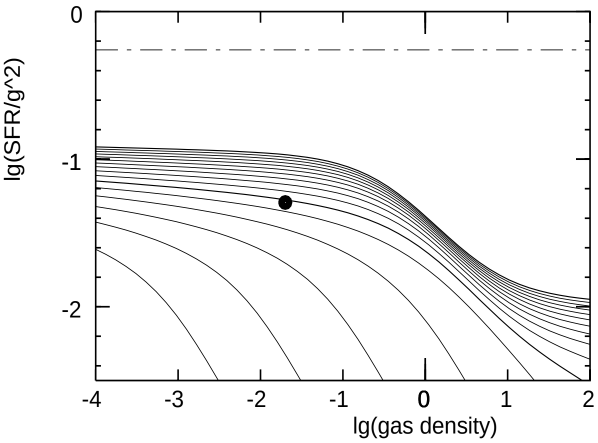

Fig. 2. Same as Fig. 1, but for an assumed linear SBF $\Psi = C_1 g f(T)$ with various values for the constant $\log(C_2)$ = 9, 8, ... , -5 (from top to bottom, the thicker curve is for $\log(C_2)$ = 0). We show the analytical solutions only.

To summarize: the self-regulation mechanism leads to an equilibrium star-formation rate which has essentially a quadratic dependence on gas density and which is independent of both the constant C_n and the exponent n of the assumed stellar birth function. Since the rate for radiative cooling of the gas is proportional to the square of the gas density, in thermal equilibrium the SFR reaches a square-law dependence on gas density (Eq. 13).

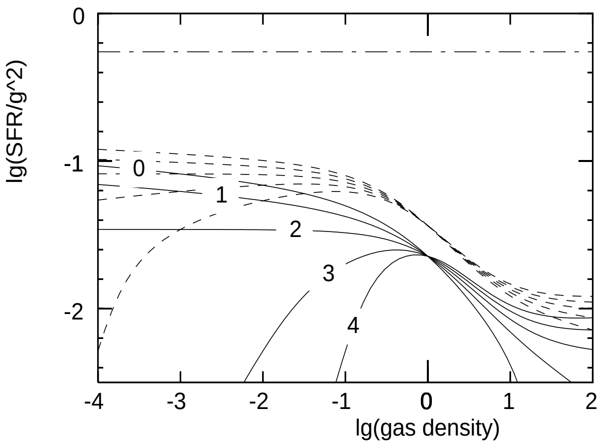

Fig. 3. Same as Fig. 1, but for various values for the power n in the assumed SBF $\Psi = C_n g^n f(T)$ and for C_n = 0.55 (full lines marked with the values for n) and $0.55 \cdot 10^6$ (dashed lines).

3.4. Sensitivity to the heating rate

Since the thermal equilibrium is important for the self-regulation via the gas temperature, the actual level of the equilibrium SFR is expected to be sensitive to both the heating rate and the star-formation efficiency factor.

First, let us consider the influence of the heating rate coefficient h. We still assume that the heating rate is proportional to the gas density, viz. h is constant. In Fig. 4 we show the equilibrium SFR as a function of gas density, for various values of h: The SFR is roughly inversely proportional to h. For low heating rates, this dependence becomes weaker, as SFR/g^2 approaches the assumed value of C_2 = 0.55. Obviously, in the absence of significant heating, the gas temperature will be close to zero, and $f(T)$ = 1. One concludes that the heating rate is a most important parameter for the temperature balance within interstellar clouds, and thus the SFR.

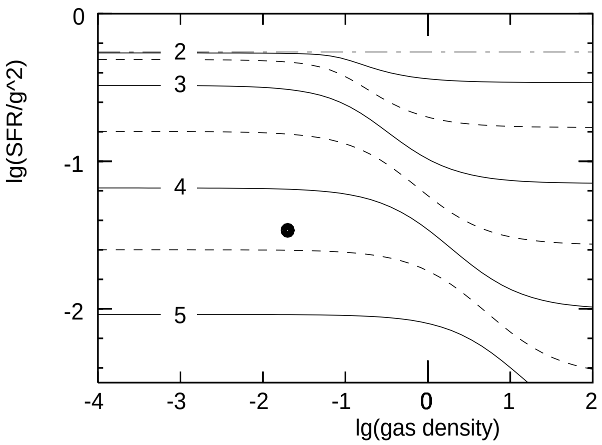

Fig. 4. Same as Fig. 1, but for various values of the heating rate coefficient h (the numbers give $\log(h)$, the filled dot indicates our 'standard' model rate h = 21900).

Let us now investigate the other (extreme) case of heating, in which the heating rate is hgs. Following the same arguments as previously, one finds a *linear* SFR:

$$\Psi_e(g, T_e) = g \frac{\Lambda(T_e)}{h\xi\tau} \quad (19)$$

which corresponds to Eq. (13), or from the condition $d(s/g)/dt = 0$ one gets the equivalent of Eq. (17):

$$\Psi_e(g, T_e) = g \frac{\Lambda(T_e)}{h\tau\xi} \frac{1 + x_e g\eta}{1 + x_e g/\xi}. \quad (20)$$

In Fig. 5 we show the equilibrium SFR/g^2 as a function of gas density for various values of C_2. Two regimes can be distinguished: if star-formation is sufficiently high to ensure self-regulation, the equilibrium SFR has a linear dependence on gas density, as described by Eq. (19). In Fig. 5 this is seen as the bunch of straight lines, falling to the right, showing that the solution is independent of the assumed value of C_2. On the other hand, low level star-formation leads to a break-down of self-regulation, and one simply has SFR/$g^2 = C_2$, as depicted in the horizontal lines in Fig. 5.

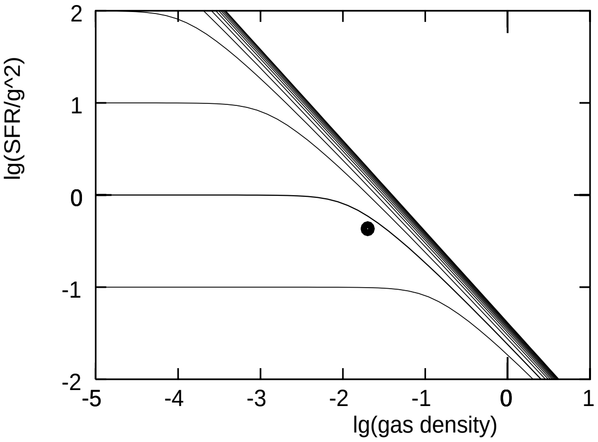

Fig. 5. Same as Fig. 1, but for a heating rate $h(g) \propto g$ depending on gas density. Shown are the solutions as C_1 is varied by factors of ten, the thick line is the curve for $\log(C_1) = 0$. The filled dot refers to $C_1 = 0.55$ at the density $n_{\rm gas} = 1$ cm^{-3}.

Finally, in Fig. 6 we show the influence of the SBF efficiency factor $f(T)$ by varying the scale temperature T_s of the exponential function. One notes that the equilibrium value of the SFR is affected by changes of T_s. However, in the framework of our scenario, the range of physically meaningful values for T_s is rather limited: In ionized gas, which is characterized by temperatures of several thousands K, star-formation is highly unlikely. It probably operates at maximum efficieny when the gas is predominantly in molecular form, i.e. for T below a few hundred K. To describe this transition of efficiency, T_s should be of the order 1000 K, within a factor of three. This corresponds to a change of the SFR of about ± 0.25 dex. Other functional forms for f(T) may be envisaged, but they should have a transition from 1 to 0 somewhere between a few hundred K and

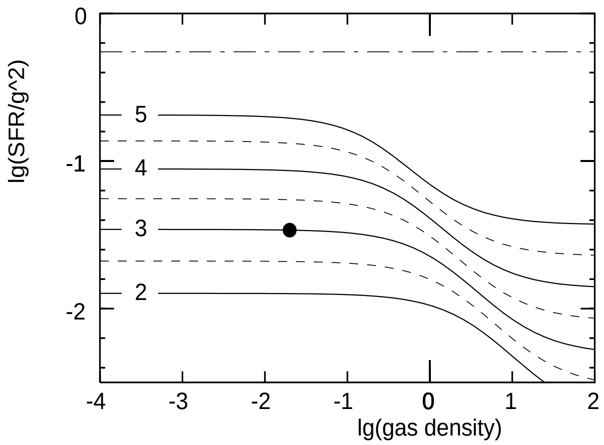

Fig. 6. Same as Fig. 1, but for various values of the temperature scale factor in the efficiency $f(T)$ of the stellar birth function. As indicated by the numbers, $\log(T_s)$ is varied from 2 to 5

several thousand K, too. Thus the influence of this function can be expected to be smaller than the dependence on the heating rate.

4. Stability analysis

The full system of Eqs. (1) to (5) describing the evolution of the physical variables (g, s, r, e) has no critical point, i.e. where all four derivatives vanish, if one ignores physically irrelevant points such as $g = s = r = 0$. However, physically relevant situations do exist where parts of the system have critical points. They are: $de/dt = ds/dt = 0$ leads to the low-density limit of the equilibrium solution Eq. (13), and $de/dt = dg/dt = 0$ which leads to the high-density limit Eq. (18). In the last section we had considered the ratio $x = s/g^2$ of stellar and gas fractions; by doing this we had essentially transformed the original system into the following set of equations which describe the evolution of (g, x, r, e)

$$g' = \frac{dg}{dt} = -\Psi + xg^2\eta/\tau \quad (21a)$$

$$x' = \frac{\Psi}{g^2}(\xi + 2xg) - \frac{x}{\tau}(1 + 2xg\eta) \quad (21b)$$

$$r' = (1 - \xi)\Psi + (1 - \eta)xg^2 \quad (21c)$$

$$e' = xg^2 h - g^2\Lambda(T) \quad (21d)$$

We note that there is only one pair of equations (21b and 21d) whose right-hand sides vanish for non-trivial parameter values. This is the equilibrium solution Eq. (17). Thus the temporal behaviour of the full system is composed of the evolution of the subsystem (x, e) around the equilibrium solution, and the overall evolution of matter from gas into remnants, which is described by Eq. (21a).

Let us investigate the stability of the system about the equilibrium solution. To do this, we may restrict ourselves to the partial system (x, e), since the relevant timescales are very different. The gas density g plays the rôle of a control parameter;

the remnant fraction has no influence on gas or star fraction or the energy. With the abbreviations (which are evaluated for our formulations as shown on the right-most column)

$$\Psi' := \frac{\partial \ln \Psi}{\partial \ln T} = -T/T_s \qquad (22a)$$

$$\Lambda' := \frac{\partial \ln \Lambda}{\partial \ln T} = 1/2 \qquad (22b)$$

one gets for the elements of the Jacobi matrix

$$\frac{\partial x'}{\partial x} = 2\frac{\Psi}{g} - (1 + 4xg\eta)/\tau \qquad (23)$$

$$\frac{\partial x'}{\partial e} = (\xi + 2xg)\frac{\Psi\Psi'}{g^3 bT} \qquad (24)$$

$$\frac{\partial e'}{\partial x} = g^2 h \qquad (25)$$

$$\frac{\partial e'}{\partial e} = -\frac{g\Lambda\Lambda'}{bT} \qquad (26)$$

The temporal behaviour of the linearized system ($x - x_e$ and $e - e_e \propto \exp(\lambda t)$) in the vicinity of the equilibrium (x_e, e_e) is characterized by the eigenvalues of the matrix, and are computed from its trace and its determinant:

$$\lambda_{1/2} = \mathbf{Tr}/2 \left(1 \pm \sqrt{1 - 4\,\mathbf{det}/\mathbf{Tr}^2}\right) \qquad (27)$$

In Fig. 7 we show for our standard model how the trace, determinant, and the discriminant $\mathbf{Disc} = 1 - 4\,\mathbf{det}/\mathbf{Tr}^2$ change with the external parameter, the gas density. This was done numerically by searching for the equilibrium point, and evaluating the Jacobi matrix elements numerically. The determinant is always positive, thus the equilibrium is never a saddle point. The trace is always negative, which means that the equilibrium is stable: i.e. the system will always return to equilibrium after any perturbation in gas density or temperature. Finally, the positive discriminant shows that for both very low and very high densities the characteristics of a node is found, so that equilibrium is approached directly. For intermediate densities, the discriminant becomes negative, which indicates that here the system performs oscillations before reaching the equilibrium. The number of oscillations that are done during one decay time is equal to $\sqrt{|\mathbf{Disc}|}/2\pi$. Since the maximum negative value for **Disc** is not much above 4, one notices that these oscillations are strongly damped.

We now investigate the stability analytically: Inserting the equilibrium solution (Eq. 17), and noting that $\Lambda/h = x$, the trace of the matrix is found to be always negative:

$$\mathbf{Tr} = -\frac{\xi + 4xg\xi\eta + 4x^2g^2\eta}{\tau(\xi + 2xg)} - \frac{g\Lambda\Lambda'}{bT} \qquad (28)$$

as long as the cooling function increases for increasing temperature $\Lambda' > 0$. Thus, the self-regulated mode of star-formation is *always stable*, irrespective of the assumed stellar birth function Ψ.

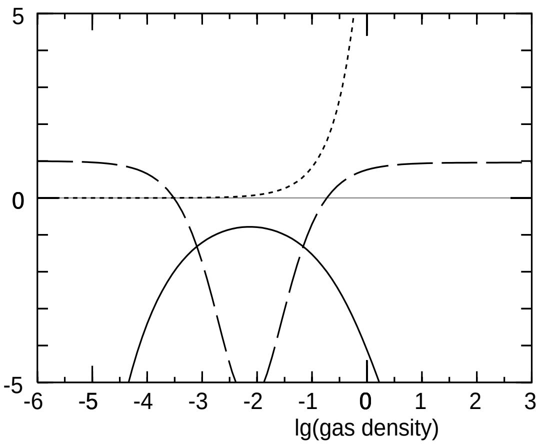

Fig. 7. Stability properties of the standard model as a function of gas density: **Tr/det** (full line), **det** (short dashes), and **Disc** (long dashes).

For the determinant one gets after some algebra using Eqs.(13) and (17), and keeping in mind that $\Psi' < 0$:

$$\mathbf{det} = \frac{g\Lambda}{bT\tau}\left(\Lambda'\frac{\xi + 4xg\eta\xi + 4x^2g^2\eta}{\xi + 2xg} + |\Psi'|(1 + 2xg\eta)\right) \qquad (29)$$

This means that the determinant is always positive, the equilibrium is either a node or a focus.

With the abbreviating definitions

$$u := \frac{g\Lambda\Lambda'\tau}{bT}$$

$$A := \frac{\xi + 4xg\eta\xi + 4x^2g^2\eta}{\xi + 2xg} \approx 1$$

$$B := \frac{|\Psi'|}{\Lambda'}(1 + 2xg\eta) \approx \frac{2T_e}{T_s}$$

one has

$$\mathbf{Tr} = -\frac{1}{\tau}(u + A)$$

$$\mathbf{det} = \frac{u}{\tau^2}(A + B)$$

and thus the discrimant is

$$\mathbf{Disc} = 1 - \frac{4u(A + B)}{(u + A)^2}$$

Thus the condition for the borderline between oscillatory and exponential behaviour $\mathbf{Disc} = 0$ is

$$4u(A + B) = (u + A)^2$$

For a sufficiently low gas density both A and B are independent of u, and so this equation can be solved for u:

$$u_{1/2} = (A + 2B)\big(1 \pm \sqrt{1 - (\frac{A}{A + 2B})^2}\big)$$

As in our standard model the equilibrium temperature is $T_e \approx T_s$ and thus $B \approx 2$, let us consider the case of $2B \gg A$ which yields:

$$u_{1/2} \approx 4B \begin{cases} 1 \\ (A/4B)^2 \end{cases}$$

and thus for the gas densities between which the system has oscillatory behaviour:

$$g_{1/2} \approx \frac{4bT|\Psi'|}{\tau\Lambda(\Lambda')^2} \begin{cases} 1 \\ (\Lambda'/4|\Psi'|)^2 \end{cases}$$

Thus the ratio of the densities $g_1/g_2 \approx (4|\Psi'|/\Lambda')^2 \approx 64$ for $T_e = T_s$. Thus the system will show oscillatory behaviour around the equilibrium solution over a range of 2 orders of magnitude in the gas density. This agrees well with the results of the numerical stability analysis (cf. Fig. 7).

These approximate expressions show: the width of the range in densities over which oscillations occur, is determined only by the temperature dependences of cooling function and star-formation efficiency. At which densities this regime is found depends on these two parameters, but also on the lifetime τ of the hot stars. For a longer lifetime the oscillatory region would be found at lower densities.

Finally, we computed various numerical models in which the system was disturbed regularily, by removing or adding various amounts of gas mass. In all these experiments, equilibrium was reached after a short (cooling timescale) transitionary interval. These disturbances never caused the system to break into sustained oscillations. This further illustrates that the self-regulated mode of star-formation indeed is a very stable process.

5. Global behaviour: The evolution before self-regulation

The global stability of the system can only be studied numerically. Since the self-regulated mode is characterized by a critical point in two variables (ratio $x = s/g^2$ of star and gas densities, and the internal energy density e) with the gas density g being a control parameter, we can study the global behaviour of the system in the (x,T)-plane. We plot T instead of e, as it allows a more convenient physical interpretation. In the following figures, we show the streamlines of the restricted system composed of Eqs.(21b) and (from Eqs.(21d,a))

$$\frac{dT}{dt} = T\Psi/g + g(x(h - bT\eta/\tau) - \Lambda)/b \tag{29}$$

at constant gas density for three values of g, depicting the typical behaviour of our standard model.

In Fig. 8 the situation at very low densities is shown. Starting at sensible initial conditions (no stars ($x = 0$) and any temperature) the system first forms stars at nearly constant temperature, because the cooling time is very long, thus making horizontal streamlines. This continues until a sufficiently large fraction of stars have been formed, i.e. when the second term on the r.h.s. of Eq. (16) is large enough. Then the system evolves following the condition $dx/dt \approx 0$ which shows up as the bunching of the streamlines along the diagonal line. The gas cools while the fraction of stars keeps increasing, until the system reaches equilibrium and enters the self-regulated mode. If the initial temperature had been below the equilibrium value, too many stars are formed first, and equilibrium is approached by heating of the gas and a decline of the stellar fraction.

Figure 9 depicts the behaviour at intermediate densities, near the centre of the oscillatory region. The tightly wound spiral shape of the streamlines shows the strongly damped oscillations which the system performs while approaching the equilibrium point. For low initial temperatures the first stage of the evolution is reminiscent of the behaviour at very low densities. At higher temperatures, the gas first cools, until the diagonal line is reached; thereafter, the evolution follows the diagonal line leading into the self-regulated mode. The strong bunching of the streamlines indicates that the final approach to equilibrium is completely *independent* of the initial conditions.

The streamlines for very high density are shown in Fig. 10. Here, oscillations are no longer present. The evolution, starting with $x = 0$ but any T, always involves a rapid cooling of the gas to very low temperatures, after which equilibrium is reached along the locus described by $de/dt = 0$ (i.e. $\Lambda(T) = xh$).

This part of the common evolution gives rise to the initial strong peak in the star-formation rate, as shown by the numerical models in Fig. 1, during which quite a large fraction of the initial gas is converted into stars and remnants. Unfortunately, the evolution of the system with the constraint of $de/dt = 0$ (or $dx/dt = 0$ for the low density case) does not lead to an analytical solution. Since the star-formation timescale in this regime is of the order of few Myrs (cf. Fig. 1), the duration of this initial evolution is rather short, quite independent of the other model parameters. Table 1 lists results from numerical models with several representative parameter values. The fraction of stars formed becomes larger, if the initial density is increased, or the heating rate is decreased, or the stellar birth efficiency factor (higher T_s) is made flatter. One notes that this fraction is independent of the both n and C_n of the assumed SBF.

Gas densities higher than about 1 $M_\odot pc^{-3}$ (hydrogen atom density 50 cm^{-3}) are somewhat difficult to imagine as the initial condition in a protogalaxy, without already undergoing star formation. It seems more likely that the gravitational collapse of the protogalactic cloud leads to a build-up of the gas density on timescales comparable to the free-fall timescale of the whole system, which is of the order of a few 100 Myr. Since the time for settling onto equilibrium (essentially the gas cooling time) is much shorter than this, one would expect that the system can reach the self-regulated star-formation quite early on, and maintain it as the gas density increases during the collapse. Thus the fraction of stars formed before and outside self-regulation could still be rather small.

6. Discussion

It should be stressed that any numerical solution of even the simple model requires some attention to numerical accuracy, as

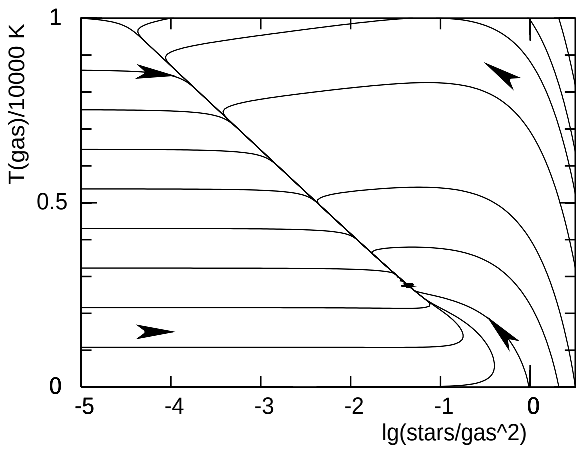

Fig. 8. Streamlines of the flow field of the system, in the x, T-plane, with a constant gas density $\log g = -4$. The equilibrium point is seen as the crowding of the streamlines into a small black spot at $\log(x) = -1.4$ and T = 2800 K.

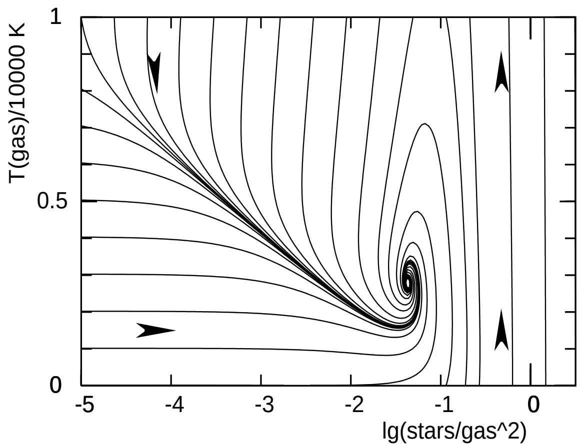

Fig. 9. Same as Fig. 8, but for a gas density $\log g = -2$.

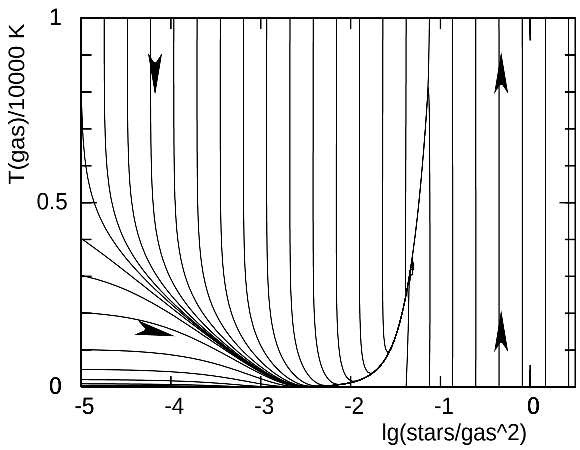

Fig. 10. Same as Fig. 8, but for a gas density $\log g = 0$. The equilibrium point is the spot at $\log(x) = -1.4$ and T = 3300 K.

the timescales of the equations vary over a large range during

Table 1. The initial evolution before the self-regulated star-formation mode is reached: given are the approximate time (in Myr) and mass fraction of stars formed in this period.

	n	C_n	$\log(g_0)$	time	fraction
	2	0.55	–1	8	0.05
	2	0.55	0	4	0.25
	2	0.55	1	4	0.65
	2	0.55	2	2	0.93
	2	55	2	2	0.91
	1	55	2	8	0.93
h = 219000	2	0.55	2	2	0.15
T_s = 100 K	2	0.55	2	2	0.65

the evolution. Especially in the oscillatory regime, the finite numerical accuracy will not permit the system to really reach the equilibrium solution. Instead it oscillates about the equilibrium with a constant amplitude, which is easily identified as a mere numerical effect due to its dependence on the integration accuracy. However, when placed into a larger, more complex network of non-linear equations, it can give rise to non-physical effects. Thus, some computational effort is necessary (cf. Theis et al. 1992).

The results of our restricted system can be compared with those from the full description applied to a closed-box model (cf. Sect. 3 of Theis et al. 1992), as well as from calculations with an intermediate model with 2 gas phases. In general, we find that whenever the more complex model is in the self-regulated mode, its SFR follows our analytical equilibrium solution rather closely. Thus the ratio Ψ/g^2 depends essentially on the *current* gas density. The main difference to our simple treatment is that the full model may enter an oscillatory mode (cf. Fig. 7 of Theis et al.) during which the SFR changes about the value expected for self-regulation periodically, but not symmetrically: The flat top part of the SFR 'pulses' in that figure corresponds to the self-regulated SFR in that model.

That the full models are seen to exhibit self-regulated behaviour is not very surprising, because as it was shown in Sect. 4 the simplified system is *always stable*. From Eq. (28) one recognizes that this applies not only to different evolutionary states but also to different parametrizations of the rates in our system. For instance, the choice of the SBF does not affect the stability condition at all. In an effort to find unstable situations, we have done numerous numerical calculations while experimenting with various parametrizations and using extreme values for the constants, but we find the (simple) system to be very robust indeed.

Full 2-dimensional calculations of the chemodynamical evolution of rotating galaxies are in progress (cf. Samland et al. 1994). Inspection of the results show that most of the volume elements are in the self-regulated mode for most of the time. Despite the varying evolutionary state of the gas in different regions of the galaxy model, the ratio $\Psi/\rho_{gas}^2 \approx 0.01 \mathrm{M}_\odot^{-1}\ \mathrm{Gyr}^{-1}$ is constant within a factor of 2. This value is only a factor 3 lower than our equilibrium value (cf. our Fig. 2), despite the different description of the processes in the ISM used by Samland et al. in comparison with the formulation of Theis et al.

In our basic model, the self-regulation is the consequence of the local heating of the gas by the stars, and its main signature is the quadratic SFR. The results of Samland et al. also show this behaviour on a more global scale, which is revealed by integrating the SFR over the height above the galactic plane and compare it to the gas surface densities: the ratio $\int \Psi dz/\Sigma_{gas}^2 \approx 0.02 \mathrm{M}_\odot{}^{-1}\ \mathrm{Gyr}^{-1}$ is fairly constant (within a factor 4) for all radii and all times. From this we expect that chemodynamical models of galaxies tend to show a quadratic SFR, corresponding to the low density regime of our analytical equilibrium solution.

We note that quadratic SFRs may also be produced in other scenarios. However, either the predicted absolute rate is incompatible with observational evidence, or essential parameters in the model are adjusted to fit the observations: The limiting value for the SBF derived by Cox (1983) from the balance of stellar ionizing photons and recombinations in the ISM yields the same dependence, however the equilibrium rate is about 30 times higher than the present SFR in the Milky Way. Franco & Shore (1984) estimate a steady state SFR from the requirement that the ISM is nearly covered by the overlapping shells blown by winds of OB stars. The exponent of the density dependence should be in the range from 1.5 to 2. However, the rate still depends on properties of the present state of the ISM. Firmani & Tutukov (1992) consider the balance of the turbulent energy of the gas, heated by supernova explosions and cooled by turbulent dissipation. Their analytical considerations yield a stationary solution, which corresponds to the total gas mass of the galaxy remaining constant, with SFR $\propto \Sigma_{gas}^{5/2}$ or Σ_{gas}^3. The resultant star-formation timescale is much too short to explain the nearly constant SFR in irregular galaxies. They suggest gas infall into galaxies may be the process limiting the SFR. Numerical models which take into account a greater number of details of the physics of stars and the interstellar medium, are found to be in very good agreement with the data of Donas et al. (1987), and consistent with a quadratic density dependence.

Observational evidence is less clear, but seems to point more towards a linear SFR. Determinations of the SFR from ultraviolet photometry of spiral and irregular galaxies by Donas et al. (1987) show that the SFR integrated over the whole galaxy is closely correlated with the total gas mas (as measured by H I 21 cm emission) with an exponent of 1.15; the SFR per unit area as a function of H I surface density shows quite a strong scatter, but is also a linear law. This is somewhat in contrast to the findings of Talbot (1980), confirmed by Rana & Wilkinson (1986) that in our Galaxy the SFR is correlated with the surface density of molecular hydrogen, with an exponent of 0.94 ± 0.39, while it is essentially independent of H I surface density. Rana & Wilkinson (1986) show that this holds true for the dependence on volume density as well. Several studies of individual external galaxies give exponents of the dependence on surface density: 1.84 ± 0.14 (SMC, Sanduleak 1969), 2.05 ± 0.1 (M31, Einasto 1972), 2.09 ± 0.16 from blue stars and 2.35 ± 0.26 from H II regions (M33, Madore et al. 1974). For the inner part of M33 Madore et al. suggest a value of less than 1. However, Wilson et al. (1991) find that the Hα luminosity and hence the SFR is nearly constant in molecular clouds in the centre and along a spiral arm, i.e. independent of the mass of gas in molecular or atomic form. Only complex no. 5 – which is a dilute feature in the interarm region – exhibits lower emission (factor 4).

The quadratic SFR is not a feature unique to the chemodynamical treatment, as discussed above. Likewise, if we assumed that the heating rate is also proportional to the gas density, a linear dependence of the SFR follows (Eq. 20). But it should be stressed that while other scenarios consider a priori a balance between two physical processes and work out the consequences, the self-regulated equilibrium is an outcome of our modeling of the interstellar medium.

7. Conclusions

We have investigated a simplified version of the network of interactions between stars and gas, as they are described in the chemodynamical approach to galaxy evolution. This restricted system is used to represent the self-regulation of star-formation within the star-forming clouds by means of the radiation from massive stars only. As the gas is heated by this radiation, the higher temperatures imply a smaller fraction of molecular gas, and hence a smaller star-formation efficiency.

The negative feedback in this system gives rise to an equilibrium solution, which is characterized by the gas being in thermal equilibrium. As a consequence, the star-formation proceeds at a self-regulated rate, which is essentially proportional to the square of the gas density, highly independent of what is assumed for the SBF (i.e. its exact dependence on gas density and temperature). In particular, it is insensitive to the factor of proportionality. For our simplified system, the equilibrium rate can be computed quite easily by solving a non-linear equation.

Under realistic conditions in galaxies and proto-galaxies, this equilibrium is reached quickly: the timescale is determined by how fast the thermal balance can adjust itself, and thus is determined essentially by the cooling time of the interstellar gas. For the present condition of the interstellar medium in the solar vicinity (with a mean density of about 1 cm^{-3}) this time is about 0.3 Myrs compared to star-formation timescale of several Gyrs. For a quadratic SBF, this is true for all gas densities.

The equilibrium rate depends quite strongly on the stellar heating rate and thus is determined by the dominant heating processes. The ionizing radiation from massive stars produces H II regions; this phase transition of the gas requires a different treatment than in the present approach. Also, the spatial distribution of clouds and gas in the ISM is quite inhomogeneous which raises the question of how the spatial average of the heating rate is computed appropriately. In the present study we have not addressed these topics which are to be done separately.

We have investigated the stability of the equilibrium solution against disturbances in the gas temperature, or the ratio of stars and gas. A linear analysis shows that the system is stable for a wide range in all the model parameters. The character of how the system reaches equilibrium changes with gas density: both for very low and very high densities, the system returns directly to equilibrium, without any oscillations. For intermediate densities ($\log(g) \approx -2$) the system will perform oscillations around the equilibrium solution. Under physically realistic conditions, these oscillations are highly damped, so typically the system settles back within a few oscillations after a disturbance. Because of this focus structure, in a numerical calculation the equilibrium solution is not reached, as due to the finite integration accuracy the solution oscillates around equilibrium. In the framework of more complex models, these might cause difficulties, unless proper attention is paid.

The global behaviour of the system, before it reaches equilibrium, has also been looked at. This is a rather short transitionary period, lasting for a few Myrs, and it is of little consequence for the further evolution of a galaxy. Only at very high densities appreciable effects occur, but in this regime the assumptions for our simple model are no longer appropriate anyway.

More complex models that use the full network of processes are seen to exhibit self-regulated behaviour most of the time, and in most parts of the model galaxy. As a consequence, we expect from the present study that the results of these model calculations will not be overly sensitive to the nature of the stellar birth law. The feature of a quadratic dependence of the SFR on gas density is preserved in these models, not only locally, but also when surface densities are considered. This is in qualitative agreement with the SFRs determined from observations in spiral galaxies. We are tempted to conclude that real galaxies have indeed some degree of self-regulation.

Acknowledgements. We thank J.S.Gallagher and M.Samland for fruitful discussions. J.K. thanks the Observatoire de Strasbourg for the warm hospitality during a stay when this manuscript was shaped into its final form. Financial support from the Deutsche Forschungsgemeinschaft is gratefully acknowledged (He 1487/13 (J.K.) and He 1487/4 (C.T.)).

References

Böhringer H., Hensler G., 1987, A&A, 215, 147
Cox D.P., 1983, ApJ, 265, L61
Dopita M.A., 1985, ApJ, 295, L5
Donas J., Deharveng J.M., Laget M., Milliard B., Huguenin D., 1987, A&A, 180, 12
Einasto J., 1972, ApL, 11, 195
Firmani C., Tutukov A., 1992, A&A, 264, 37
Franco J., Cox D.P., 1983, ApJ, 273, 243
Franco J., Shore S.N., 1984, ApJ, 285, 213
Guibert J., Lequeux J., Viallefond F., 1978, A&A, 61, 1
Hausman M.A., 1981, ApJ, 245, 72
Hensler G., 1987, Mitt.Astron.Ges. 70, 141
Hensler G., Burkert A., 1989, Proc. Erice Workshop "Windows on Galaxies", eds. G.Fabbiano et al., Reidel, Dordrecht, p.321
Hunter D.A., Gallagher J.S., 1985, ApJS, 58, 533
Köppen J., Arimoto, N., 1990, A&A, 240, 22
Larson R.B., 1969, MNRAS, 145, 405
Larson R.B., 1982, MNRAS, 200, 159
Madore B.F., van den Bergh S., Rogstad D., 1974, ApJ, 191, 317
McKee C.F., Ostriker J.P., 1977, ApJ, 218, 148
Rana N.C., Wilkinson D.A., 1986, MNRAS, 218, 497
Samland M., Hensler G., Theis, Ch., 1994, in preparation
Sandage A., 1986, A&A, 161, 89
Sanduleak H., 1969, AJ, 74, 74
Schmidt M., 1959, ApJ, 129, 243
Tenorio-Tagle G., Bodenheimer P., Lin D.N.C., Noriega-Crespo A., 1986, MNRAS, 221, 635
Theis C., Burkert A., Hensler G., 1992, A&A, 265, 465

This article was processed by the author using Springer-Verlag TEX A&A macro package 1992.